Diaphragm based optical fiber sensor for pulse wave monitoring and cardiovascular diseases diagnosis

Jingyi Wang[1, †], Kewei Liu[1, †], Qizhen Sun[1,*], Xiaoling Ni[2], Fan Ai[1], Senmao Wang[1], Zhijun Yan[1], Deming Liu[1]

[1] School of Optical and Electronic Information, Wuhan National Laboratory for Optoelectronics, and National Engineering Laboratory for Next Generation Internet Access System, Huazhong University of Science and Technology, Wuhan 430074, Hubei, P. R. China

[2] Hospital of Huazhong University of Science and Technology, Wuhan 430074, Hubei, P. R. China

* Corresponding author.
E-mail address: qzsun@mail.hust.edu.cn (Q. Sun).

[†] These authors contributed equally to this work.

Keywords: Optical fiber sensor; Biomedical sensor; Diaphragm; Non-invasive measurement; Pulse wave diagnosis.

Abstract

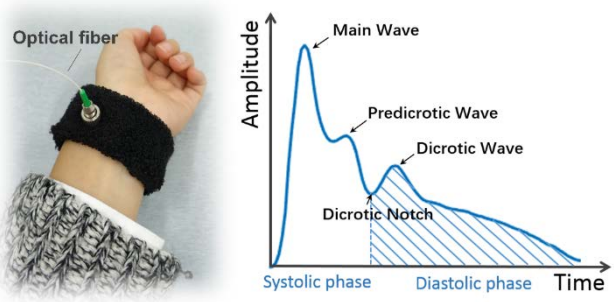

Arterial pulse wave has been considered as a vital sign in assessment of cardiovascular diseases. Non-invasive pulse sensor with compact structure, immunity to electro-magnetic interference and high sensitivity is the research focus in recent years. While, optical fiber biosensor is a competitive option to meet these needs. Here, a diaphragm based optical fiber pulse sensor was proposed to achieve high-precision radial pulse wave monitoring. A wearable device was developed, composed of a sports-wristband and an aluminum diaphragm based optical fiber sensor tip of only 1cm in diameter, which was highly sensitive to the weak acoustic signal. In particular, coherent phase detection was adopted to improve detection signal-to-noise ratio (SNR), so as to recover the high-fidelity pulse

This article has been accepted for publication and undergone full peer review but has not been through the copyediting, typesetting, pagination and proofreading process which may lead to differences between this version and the Version of Record. Please cite this article as doi: 10.1002/jbio.201900084

waveforms. A clinical experiment was carried out to detect and morphological analyze the pulse waveforms of four subjects, the results of which preliminarily demonstrated the feasibility of pulse diagnosis method. The proposed pulse fiber sensor provides a comfortable way for pulse diagnosis, which is promising in early cardiovascular diseases indicating.

1. Introduction

Pulse diagnosis is an important tool in Traditional Chinese Medicine (TCM). Some researches have shown that the morphological characteristics of pulse wave are closely related to the arterial pulsatile function [1]. The waveform in a pulse cycle can reflect the heart pumping characteristics, in which the position of systolic peak and inflexion are often related with the appearance of arterial stiffness, obstruction or cardiac disease. Therefore, the detection and analysis of pulse waveform are of great significance to early diagnosis of cardiovascular diseases, especially for asymptomatic people. The pulse signal can be regarded as the weak acoustic signal on vascular wall or skin surface. However, it is weak and full of details, requiring high precision measurement technique to achieve reliable pulse evaluation.

Much work has been done in the study of pulse wave sensors, and the schemes are basically divided into non-contact and contact types. Non-contact pulse sensing systems provide remote vibration monitoring by optical means. Image sensors based on CMOS [2], CCD [3], and infrared sequence images [4] have been developed to obtain pulse information. And continuous blood pressure detection has been achieved via non-contact two-point defocused imaging on chest and wrist [5]. Although non-contact detection can

provide continuous and more comfortable diagnosis for patients, the measurement stability and precision are not satisfactory due to the environmental noise and inevitable movement of patients. While, pulse sensors of contact type are popular for the simple structures and high signal to noise ratio (SNR). Among them, Photoplethysmogram (PPG) is a low-cost optical technique that depicts pulse waveform by detecting blood volume changes in the microvascular bed of tissues [6]. However, the depth insensitivity is a common problem of PPG sensors. The measured PPG signal is usually mixed with pulsation components of different blood vessel types, which may lead to inaccurate physiological measurement results. Further improvements have emerged, including multi-wavelength method for arterial pulse extraction [7] and implantable PPG sensor of hundred microns to monitor arterial distension directly [8]. Besides, electronic sensors have been studied thoroughly, which can be made into wearable device [9] or home-use diagnostic equipment [10]. Some are capable in multichannel detection, such as arterial tonometer [11] and Polyvinylidene Fluoride (PVDF) based piezoelectric sensor [12,13]. Unfortunately, the electrical element suffers from electro-magnetic interference (EMI).

Optical fiber sensor is newly developed biomedical sensor, which presents significant advantages as a medical equipment [14]. Firstly, the optical fiber has excellent immunity to EMI, allowing the real time monitoring of physiological acoustic signals simultaneously with the use of electrical cauterization tools, such as magnetic resonance imaging (MRI), or other examination procedures. Secondly, it is small and

biocompatible, which makes it safer for patient and easier to sterilize. Finally, optical fiber sensor has ultra-high measurement sensitivity, so as to provide more detailed pulse information to ensure the diagnostic accuracy. There are kinds of fiber pulse sensors reported. The hetero-core fiber based sensor has been found sensitive to moderate bending, so that designed to detect the minimum pulse pressure from the radial artery at the wrist [15]. Leitão et al. have proposed a simple and cheap plastic optical fiber sensor for carotid pulse waveform monitoring [16], where the pulses of three subjects are measured. Meanwhile, an ultra-short distributed Bragg reflector (DBR) fiber laser has been used as pulse sensing element [17], which has the potential to be embedded into textile.

In this work, we proposed a diaphragm based fiber pulse sensor to provide high-precision pulse wave monitoring. The sensor tip was made of an aluminum diaphragm and a fiber pigtail, with about 1cm in diameter. Wrist radial artery was chosen as measurement site and the fiber sensor tip was embedded into a sports-wristband to form a wearable device. With the help of coherent phase detection techniques, high-fidelity pulse waveforms were recovered. Further, the proposed miniature and highly sensitive sensor provided a comfortable way for pulse diagnosis. We tested the pulse waveform of four subjects by the developed system, and then quantitatively analyzed the pulse morphological parameters in time domain. By comparing the pulse analysis results with physical examination reports, the feasibility of pulse diagnosis by optical fiber sensing

system was preliminarily verified, showing great potential in early cardiovascular diseases indicating.

2. Methods

2.1 Sensing principle

The proposed pulse sensor tip consisted of an optical fiber pigtail and an aluminum diaphragm. The probe laser injects through the single mode fiber (SMF) pigtail, reflected by the aluminum diaphragm, and then coupled back into the fiber. When acoustic wave is introduced, the diaphragm will be periodical deformed, causing the optical phase of reflected light to change. The scheme of optical fiber pulse sensor is depicted in Fig. 1(a). As mentioned in reference [18], the relationship between diaphragm deflection h and the applied pressure P induced by pulse wave can be established as Eq. (1), while the corresponding optical phase change $\Delta\varphi$ is expressed as Eq. (2).

$$h = \frac{3(1-\upsilon^2)d^4}{256Et^3}P \tag{1}$$

$$\Delta\varphi = \frac{2\pi h}{\lambda} \tag{2}$$

Where d and t represent the diameter and thickness of the aluminum diaphragm, υ and E are respectively the Poisson ratio and Young's modulus of the diaphragm, λ is the wavelength of probe laser. There is a linear relationship between the optical phase change $\Delta\varphi$ and acoustic pressure P from pulse signal. Besides, equation (1) shows that the

sensitivity is inversely proportional to the cube of the thickness *t* of diaphragm. For that reason, a thin aluminum diaphragm of only 12 μm was adopted, to provide higher sensitivity and meanwhile robust to touch the human skin directly.

As we know, heart pumps blood and generates pressure signals in the artery, reflecting in the regular expansion of blood vessel walls. This pressure wave is also described as the "pulse wave", which is a kind of acoustic signal with low frequency, exists in the aorta, carotid artery, and limbs artery. It travels to the surface of the skin and is detected by non-invasive fiber sensors, as shown in Fig. 1(b). By touching the wrist skin, the diaphragm conducts atrial acoustic signals to the sensing fiber and modulates the optical phase of reflected light. The reflected detection light is transmitting through the flexible optical fiber, bound in the fiber core and carried with pulse wave information.

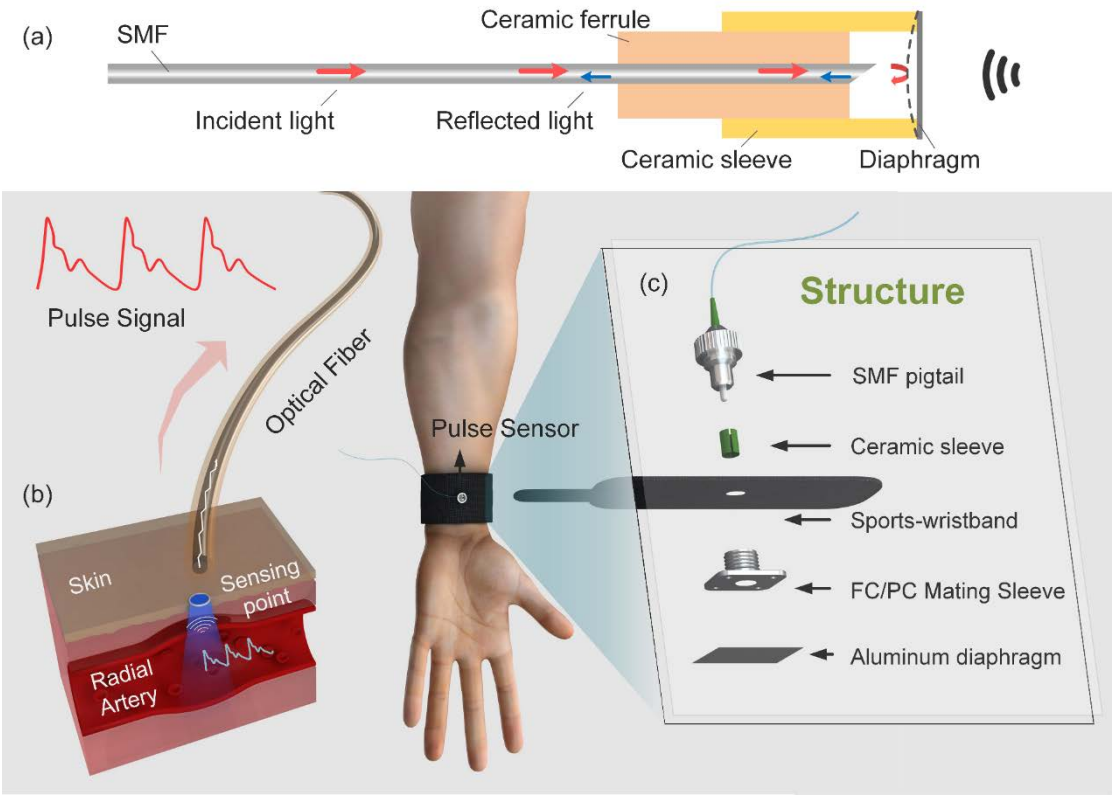

Fig. 1. (a) Schematic diagram of optical fiber pulse sensor; (b) Structural design of wearable pulse sensor; (c) The transmission of pulse waves signals.

2.2 Fabrication of wearable pulse sensor

The radial artery was chosen as the pulse monitoring location due that the support of the radius facilitates the fixation of contact pulse sensor [19]. As described in Fig. 1(c), a wearable device based on sports-wristband was fabricated with the width of 4 cm. The optical fiber pigtail was made of a SMF of 9/125/250 μm (fiber core/cladding/coating diameter) with flexible rubber case of 0.9 mm in diameter, a ceramic ferrule with an outer diameter of 2.5 mm, and a metal base with a 1 cm diameter inner thread for fixation. The

facet of SMF was polished with an angle of 8° to reduce the Fresnel reflection from the fiber end. A side-opening ceramic sleeve with the diameter of about 3mm was tightly assembled to the SMF pigtail, for the protection of fiber end. A small hole was cut in the sports-wristband, where a FC/PC mating sleeve with external thread was fixed on one side. The SMF pigtail with ceramic sleeve was threaded tightly onto this mating sleeve from the other side of the wristband, making the structure stable. A 1.5 cm *1.5 cm aluminum diaphragm of 12 μm in thickness was glued to the top of the mating sleeve for acoustic sensing. Make sure the diaphragm of the pulse sensor tip was fixed around the radial artery. And the sports-wristband was used to adjust the location of sensing point and the tightness of compression, according to the different conditions of patients.

2.3 Experimental setup

Coherent phase demodulation technique was employed to improve the detection SNR of optical fiber pulse sensor, which up-converted the signal onto the high sideband frequency to reduce the noise. It helped to achieve accurate pulse measurement with low computation complexity. The pulse diagnosis system is shown in Fig. 2(a), while its experimental setup is illustrated schematically in Fig. 2(b). The light source in this demodulation system was a continuous wave (CW) laser with narrow linewidth (Koheras BasiK, NKT Photonics, Denmark), with the wavelength of 1550nm. The laser was split into the probe light and the local-oscillator light by 99:1. The probe light was modulated

into light pulses with the width of 20 ns through a fiber-coupled acoustical optical modulator (AOM, T-M200-0.1C2J-3-F2S, Gooch&Housego, UK), as well as being frequency shifted by 200 MHz. The repetition rate of light pulse was defined here as the optical sampling rate, which was set to be 100 Hz. After amplified by an erbium-doped optical fiber amplifier (EDFA), the probe light pulses launched into the sensing fiber through a circulator. The sensing fiber consisted of a fiber Bragg grating (FBG) of 5% reflectivity and the pulse sensor tip, connected with SMF delay line (DL) of about 5m. Note that the FBG here was served as a referenced reflection point with fixed optical phase. The injected light pulses were first partly reflected by FBG and then by aluminum diaphragm of pulse sensor tip, and the two reflected pulses interfered with local-oscillator light successively. The generated beat frequency signals were received by a balanced photo detector (BPD, PDB480C-AC, Thorlabs, USA) and collected by a Data acquisition card and FPGA module (NI 5781& NI 7962, National Instrument, USA), with sample rate of 2GS/s.

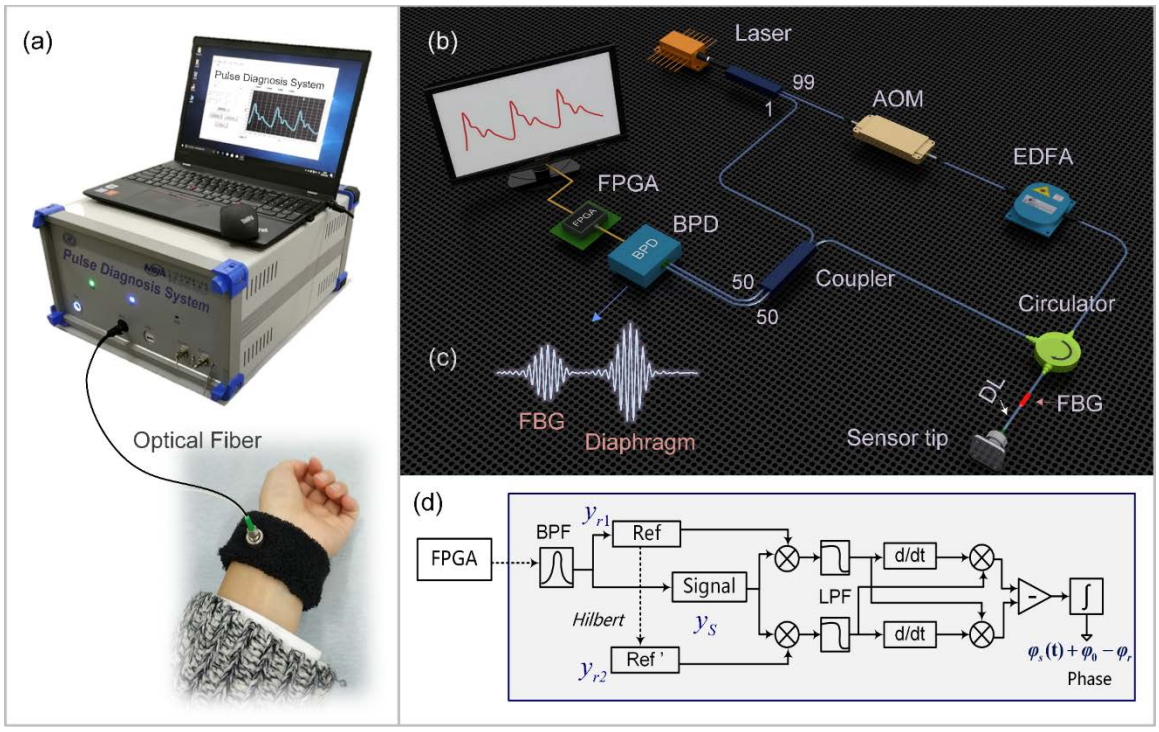

Fig. 2. (a) Photograph of pulse diagnosis system; (b) Experimental setup for pulse pressure sensing; (c) Beat frequency signals; (d) The flow chart of digital IQ demodulation.

The beat frequency signal received by FPGA acquisition module can be expressed as:

$$I = I_1 + I_2 + 2\sqrt{I_1 I_2}\cos(2\pi\Delta f t + \varphi_s(t) + \varphi_0) \quad (3)$$

Where I_1 and I_2 are the intensities of probe light and the local-oscillator light, Δf is the frequency-shift of the probe light, $\varphi_S(t)$ represents the phase change induced by the signal to be measured, and φ_0 is the initial phase difference between the probe light and local-oscillator light. Due to the different time delay of reflected light pulses, beat

frequency signals from FBG and aluminum diaphragm could be distinguished in time domain, as shown in Fig. 2(c). The optical phase information was further extracted through the digital signal processing algorithms [20], in which the processing time for a typical cycle was less than 10μs. The flow chart of demodulation process is shown in Fig. 2(d). A band pass filter (BPF) was used to extract the intermediate frequency (IF) component, and the filtered signal could be expressed as:

$$y_S = B\cos\left[2\pi\Delta f + \varphi_S(\mathrm{t}) + \varphi_0\right] \tag{4}$$

The phase change $\varphi_S(\mathrm{t})$ induced by pulse signal can be extracted by digital in-phase (I) and quadrature (Q) demodulation process. And in this work, the reflection signal from FBG was used as one of the orthogonal reference y_{r1}, while the other reference y_{r2} was generated by *Hilbert* transform.

$$\begin{cases} y_{r1} = C\cos\left[2\pi\Delta f t + \varphi_r\right] \\ y_{r2} = C\sin\left[2\pi\Delta f t + \varphi_r\right] \end{cases} \tag{5}$$

Signal y_S was multiplied by the reference orthogonal signal y_{r1} and y_{r2}, and then low-pass filtered to obtain a pair of orthogonal signals. After the differential cross-multiplying (DCM) and integration process, the optical phase was extracted.

$$\varphi = \varphi_S(\mathrm{t}) + \varphi_0 - \varphi_r \tag{6}$$

Further, optical phase change between the FBG and the diaphragm of sensor tip was calculated as equation (7).

$$\Delta\varphi=\left[\varphi_S(t)+\varphi_0-\varphi_r\right]-\left[\varphi_{S0}+\varphi_0-\varphi_r\right]=\varphi_S(t)-\varphi_{S0} \quad (7)$$

Where the φ_{S0} represents the optical phase of FBG. It can be seen that the FBG here eliminated the phase noises from light source or other disturbance on optical fibers in the demodulation terminal. Meanwhile, the fiber delay line was coiled and protected in an acoustic shield from the irrelevant environmentally vibration.

However, the direct current (DC) drift error existed in raw data, which was mainly attributed to the movement of wrist during measurement. In Fig. 3, the pulse signal of a 24-year-old male in 20 seconds is shown. High-fidelity pulse waveform was recovered with raw data and without any filtering process. And after high-pass filtering process, the de-noised pulse signals showed better uniformity. Heart rate was calculated to be 66 beats per minute. Pulse cycles could be clearly visible, where all detailed characteristics were exhibited, including the systolic peak, inflexion, dicrotic notch and the dicrotic peak [14].

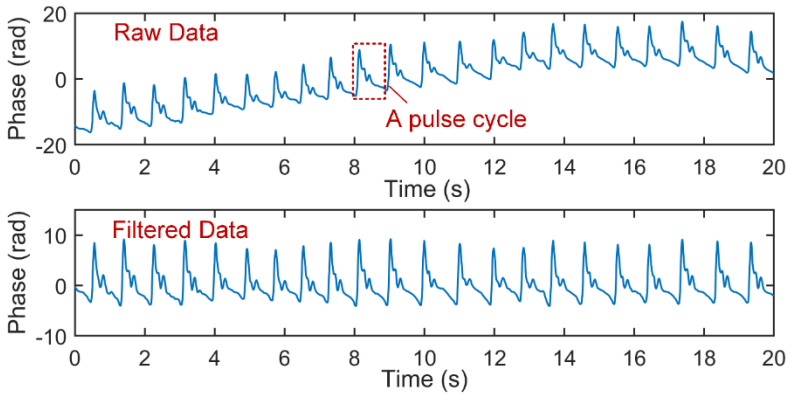

Fig.3. Pulse waveforms of a 24-year-old male, before and after high-pass filtering.

2.4 Experimental protocol

Four subjects aged between 22 and 24 years old volunteered for the clinical experiments of pulse diagnosis and cardiovascular assessment. Their basic information is listed below.

Table 1. Basic information of participants in the clinical

Subject	Gender	Age	Height (cm)	Weight (kg)	Blood pressure (mmHg)
A	Male	24	177	54	110/70
B	Male	22	180	66	104/65
C	Male	22	172	100	128/80
D	Female	24	156	46	124/72

The volunteers were asked to sit quietly until the heart rate and blood pressure are stable, in which the blood pressure is measured three times by an electronic sphygmomanometer (Omron HEM-7124). Then wear the wristband-like pulse sensor at the right-hand-side radius of the patients' wrists. Make sure the diaphragm of the pulse sensor tip was fixed around the area where the pulse was strong. The real-time pulse wave monitoring for 20 seconds were carried out. Record the amplitudes of the three characteristic peaks in pulse waveform, including the main wave, predicroti wave and dicrotic wave, so as to calculate the pulse parameters and evaluate the health condition of subjects.

Besides, for validation and comparison purposes, related cardiovascular examinations were carried out in Huazhong University of Science and Technology Hospital (Wuhan, China) and Hubei Provincial Hospital of TCM (Wuhan, China).

2.4.1 Pulse diagnosis method

The morphological characteristic of pulse waveform in time domain is regarded as the best clinical indicator to diagnose cardiovascular diseases [1], such as early vascular damage or reduced arterial compliance. As shown in Fig. 4, a typical pulse waveform of the 24-year-old male has been plotted. The pulse cycle is generally divided into systolic phase and diastolic phase, the junction of which is called the dicrotic notch. In systolic phase, the blood is pumping from heart, results in a sharp rise in blood pressure, corresponding to the main wave in pulse waveform. And the predicrotic wave is formed by the multiple reflections of arterial wall. In diastolic phase, the aortic valve closes. The elasticity of the vessels causes a small amount of blood pumping back to the heart, creating a brief rise in blood pressure, appearing as dicrotic wave.

The method for pulse waveform contour analysis varies greatly, but equally satisfactory in result. Researchers used “combined parameters” to evaluate artery compliance and peripheral resistance from the waveform [21], including H2/H1, H3/H1, H4/H1 and S1/ (S1 + S2), etc. [22,23]. Where the H1-H4 represents the height of systolic peak, inflexion, dicrotic notch and the dicrotic peak, respectively, S1 and S2 are the area of systolic phase and diastolic phase.

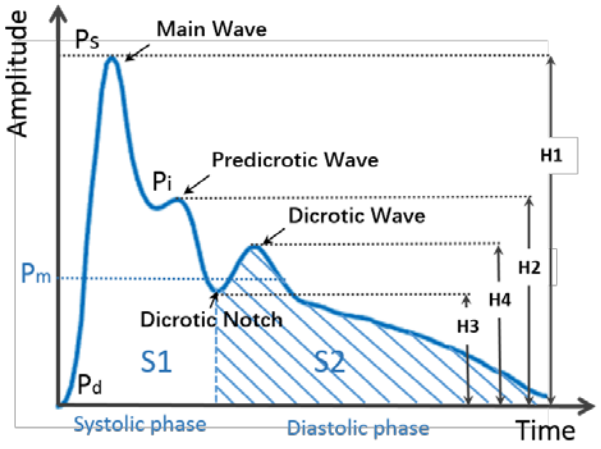

Fig. 4. The waveform of one pulse cycle

In this work, we adopted a widely-used assessment indicators [24] named augmentation index (AIx), as well as some more specific assessment formulas demonstrated in references [25-28]. The clinical empirical formula we used for pulse diagnosis are listed as follows.

(a) Mean blood pressure (MBP)

The average blood pressure in artery, marked as *Pm* in Fig. 4. It is calculated according to the morphological parameter of pulse waveform, together with the measured systolic blood pressure (SBP) and diastolic blood pressure (DBP).

$$P_m = \frac{1}{T}\int_0^T P(t)dt \qquad (8)$$

(b) Heart Rate (HR)

The number of beats per minute in quiet state. HR is inversely proportional to the pulse cycle *T*. And the reference HR of a healthy person is between 60 and 100 beats per minute.

(c) Augmentation Index (AIx)

A commonly used indicator in pulse waveform analysis.

$$AIx = \frac{P_i - P_S}{P_S - P_d} \quad (9)$$

Where *Ps*, *Pd*, and *Pi* respectively refer to the SBP, DBP and the pressure of predicrotic wave, marked in Fig. 4. The value of AIx is usually negative for young healthy people, while it increases and become positive in elder age groups. Smaller AIx value often indicates better artery compliance.

(d) K value

A morphological description index of pulse waveform.

$$K = \frac{P_m - P_d}{P_S - P_d} \quad (10)$$

Where, *Pm*, *Pd* and *Ps* refers to the MBP, SBP and DBP respectively. The K value is usually closely related to age and changes with the peripheral vascular resistance.

(e) Blood Viscosity (V)

A measure of the resistance of blood flow. The Increased blood viscosity often reflects cardiovascular diseases, such as coronary heart disease, myocardial infarction and

cerebral thrombosis. Some researches [29] suggest that the blood viscosity parameters V is closely associated with the K values. The clinically formula is given as:

$$V = K \times 11.43 \quad (11)$$

2.4.2 Gold standard method

The gold standard methods of cardiovascular physical examination in the hospital are described as follows.

(a) Electrocardiogram (ECG)

The standard 12-lead electrocardiogram (ECG) is one of the most commonly used medical studies in the assessment of cardiovascular disease, such as arrhythmias, myocardial ischemia and infarction.

(b) Arteriosclerosis level test

The arteriosclerosis level is assessed by the pulse wave velocity (PWV) index, which is a classic marker and predictor of cardiovascular risk [31]. This item involves simultaneously measurement of the arterial pulses from all four limbs, thus to calculate the pulse transmission time. The better the arterial compliance, the smaller the PWV value.

(c) Blood rheology test

Blood rheology measurement is employed to study the flow properties of blood and its elements of plasma and cells, and the blood viscosity can be measured by viscometers capable of measurements at various shear rates, such as a rotational viscometer.

3. Results and discussion

3.1 Assessment results of pulse diagnosis

As shown in Figs. 5(a)-(d), the details of pulse waveforms for 20s were restored with high-fidelity. The typical pulse cycle with the amplitude closest to average value was selected, plotted in Figs. 5(e)-(h) respectively. And the error bars were marked at the three feature position. Intensity fluctuation may exit between different pulses, which is mainly caused by the inevitable movement of the subject's wrist. However, we believe all the waveforms of pulses can be used for calculation, because the relative intensity ratio of the three feature peaks is the key parameter for cardiovascular health assessment, rather than their absolute intensity. It is interesting that pulse morphological characteristics, especially the amplitude of predicrotic wave and dicrotic wave, varied with each individual. In particular, subject A seems to had an implicit predicrotic wave. And the pulse period of subject C is observed to be irregular, as marked in Fig.5 (c), which is possibly caused by arrhythmia.

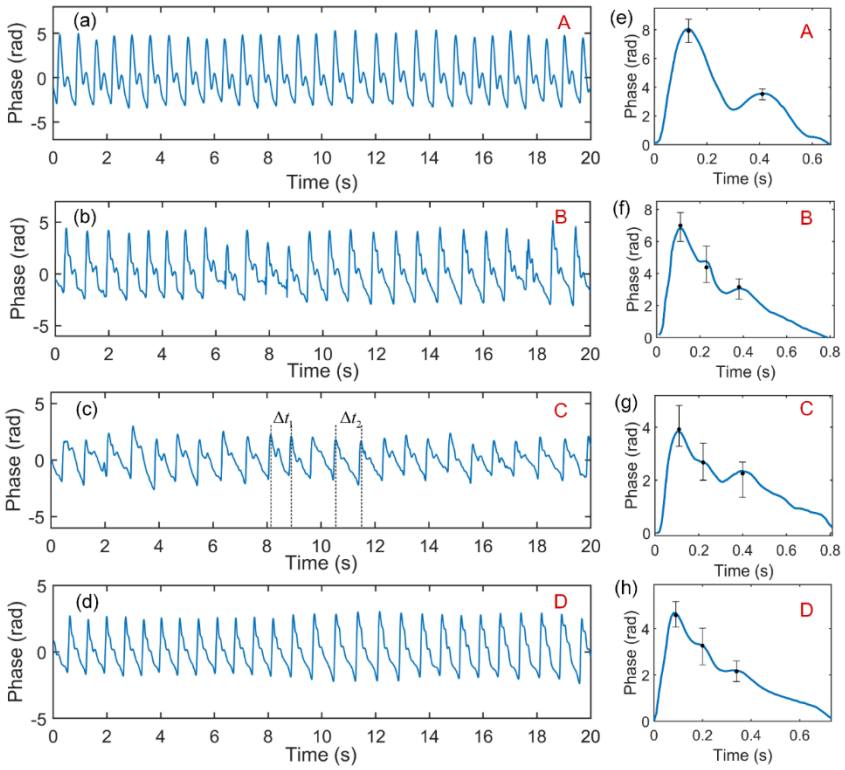

Fig. 5. Pulse waveforms (a)-(d) in 20 seconds and (e)-(h) in one pulse cycle, detected for four subjects: A – 24 years old male, B – 22 years old male, C – 22 years old male and D – 24 years old female.

For young and healthy people, the main wave of pulse signal is high and sharp. And due to the good elasticity of artery, the reflected wave of cardiac impulse will be strong and with low velocity, leading to higher amplitude of dicrotic wave and relative lower position of dicrotic notch at phase axis. Aging or atherosclerosis alters arterial pulsatile function and produces consistent changes in pulse contour. The dicrotic notch will be elevated and hard to be distinguished from the dicrotic wave. Judging from the waveforms A-D, the pulse signal of subject A has the highest main wave, together with

the lowest dicrotic notch. Beside, it has been stated in some articles that the reflection for a pretty young person only takes place in diastole phase, which consequently leads to the absence of predicrotic wave [30]. Therefore, the arterial health of subject A is believed to be the best. Comparatively, the arterial condition of C and D are not ideal enough, for the relative high dicrotic notch and the weak dicrotic wave, respectively.

Table 2. Analytical results of clinical pulse diagnosis

Indicator \ Subject	A	B	C	D
T (s)	0.69	0.79	0.83	0.73
MBP (mmHg)	85.4	80.1	102.7	92.6
HR (bpm)	87	76	72	82
K value	0.384	0.387	0.474	0.397
V value	4.39	4.42	5.42	4.54
AIx	NA	-0.303	-0.298	-0.225

To quantitatively analyze the cardiovascular health conditions of the four subjects, the pulse parameters are calculated and listed in Table 2. According to the definition above, it is believed that the lower values of the parameters K, V, and AIx mean better peripheral vascular resistance, blood viscosity, and arterial compliance, respectively. The result shows that the subject C has the maximum values of K and V among the four subjects, and D has the maximum AIx index. While, A and B have better performance on these three indicators. By analyzing the qualitative waveform contour and the quantitative parameters of the measured pulse signals, we can infer that the cardiovascular health

conditions of subject A and B are slightly better than C and D, though all of them stays healthy concerning cardiovascular conditions.

3.2 Comparison with gold-standard method

The gold-standard cardiovascular indicators of the four subjects are listed in Table 3, including blood pressure, arteriosclerosis level (PWV), electrocardiogram and whole blood viscosity. According to the electrocardiograph (ECG) results, subject C is suffering from an arrhythmia, which has also been found in our continuous pulse test for 20 seconds (see Fig. 5(c)).

Table 3. Physical examination results

Indicator \ Subject	A	B	C	D	Reference Value
Blood Pressure (mmHg)	110/70	102/70	128/80	126/68	90-140 /60-90
PWV-right (cm/s)	1066	1198	1251	1299	1000-1400
Electrocardiogram	Sinus rhythm	Sinus rhythm	Sinus arrhythmia	Sinus rhythm	Sinus rhythm
Whole blood viscosity 1.00 (1/s)	16.34**L**	15.31**L**	17.86	14.21	17.63-21.35 (13.79-17.91)*

* Blood viscosity is related to the gender, the reference value of female is in brackets

The arterial vascular health can be reflected by two indicators, arteriosclerosis level and whole blood viscosity. Intuitive comparisons of physical examination results and

clinical trial results are drawn in Figs. 6(a) and 6(b), respectively, which reflects the arteriosclerosis degree, and the blood viscosity/vascular resistance. The PWV values of all subjects are within the reference range, demonstrating that none of them suffers from arteriosclerosis. And when we do horizontal comparison between the subjects, we find that the sequence of PWV value from high to low is: D, C, B, A, in which subject D has the highest arteriosclerosis level. This is a very equivalent result by using AIx in pulse diagnosis, as shown in Fig. 6(a). The sequence of whole blood viscosity from high to low is: C, A, B, D, in which subject C has the greatest whole blood viscosity. The comparison results with the parameters K and V are shown in Fig. 6(b). However, unexpected result can be seen between subject A and B, owing that the whole blood viscosity values of A and B are extremely low to below the reference value, and thus measurement errors exist. Besides, subject D is the only female of four, and the blood viscosity of female is generally lower than that of male. The physical examination results prove that the arterial conditions of subject A and B are better than that of C and D, which is consistent with the conclusion made by our proposed method, demonstrating the measurement feasibility of pulse diagnosis method using optical fiber sensor.

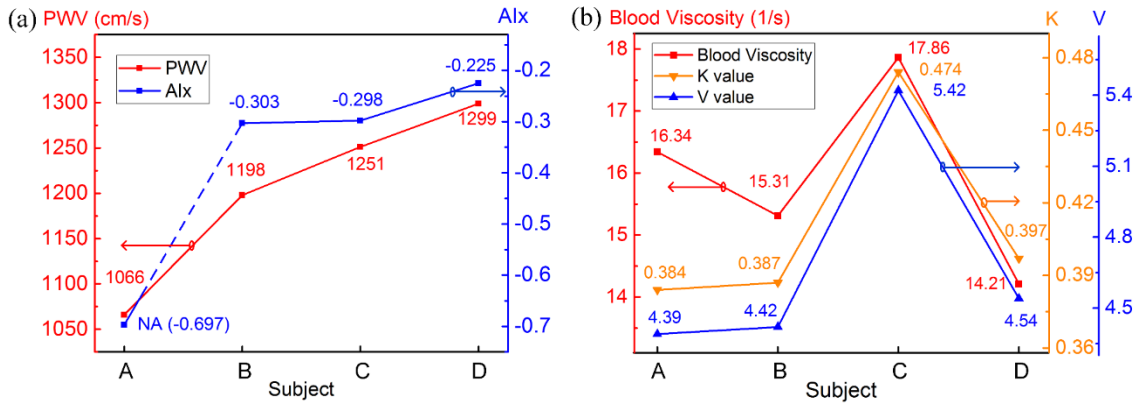

Fig. 6. Comparisons of clinical trial and physical examination toward (a) arteriosclerosis index and (b) blood viscosity or arterial resistance. Left axes: the evaluation indexs used in physical examination. Right axes: the evaluation indexs used in our clinical trial. The AIx value of subject A is not available (NA) for the absence of predicrotic wave in systolic phase, the amplitude of his dicrotic notch is adopted here instead of predicrotic wave, for calculation only.

Even for young and healthy people, visible differences can be observed in their cardiovascular indicators and pulse parameters. So we believe that the morphological change of pulse wave can be an early predictor of premature cardiovascular disease. For asymptomatic people, the proposed pulse diagnosis can effectively evaluate vascular conditions in advance and avoid the risk of cardiovascular disease. And in particular, the proposed pulse monitoring method based on optical fiber sensor is passive and noninvasive, providing a safer and more convenient way for cardiovascular diseases screening.

Further clinical experiments will be carried out in the follow-up works. Since only four subjects have participated in our clinical test for the pulse analysis, the distribution of subjects should be expanded in quantity, ages and health conditions. However, the

focus of this work is to be put forward a high-sensitive optical pulse sensor, which can provide reliable and detailed pulse waveform detection. The experimental results roughly demonstrated the potential of the proposed fiber optic pulse sensor in early assessment of cardiovascular disease. Admittedly, the size of the terminal device is large, and the cost of it is relatively high at the present stage. However, it has the capacity now to be used in the hospital to provide more comfortable pulse diagnosis. And it is expected to be made into miniaturized, low-cost and portable device with the development of optoelectronic integration technology. Besides, though experimental data is taken for only 20 seconds in this paper, the proposed technique is capable of dynamic monitoring over long period, which is suitable for the development of wearable devices. Further, the simultaneously pulse measurements for multi-person will be developed by optical fiber networking technology in the future work, to significantly improve the detection efficiency.

4. Conclusion

We have reported an aluminum diaphragm based optical fiber pulse sensor, as well as the coherent phase demodulation system to achieve radial pulse waveform detection. The sensor tip is tiny with about 1cm in diameter, which can be fixed into the sport-wristband as a wearable device. In real-time pulse monitoring, detailed characteristics of pulse wave signals, including the systolic peak, inflexion, dicrotic notch and the dicrotic peak have been restored with high-fidelity. Meanwhile, pulse waveforms of four young and

asymptomatic subjects have been collected, and quantitatively analyzed according to the pulse morphological parameters. The pulse analysis gave an equivalent conclusion with the cardiovascular assessment in hospital. The proposed optical fiber pulse sensor can provide a safer and more convenient option for early diagnosis of cardiovascular disease.

Acknowledgements

This work was financially supported by National Natural Science Foundation of China (NSFC) (61775072); National Key Research and Development Program of China (2018YFB2100902); Science Fund for Creative Research Groups of the Natural Science Foundation of Hubei (2018CFA004); Major projects of technical innovation of Hubei (2018AAA040); Fundamental Research Funds for the Central Universities (2017KFXKJC002, 2019kfyRCPY095).

References

[1] G. E. McVeigh, C. W. Bratteli, D. J. Morgan, C. M. Alinder, S. P. Glasser, S. M. Finkelstein, and J. N. Cohn, *Hypertension* **1999**, 33(6), 1392.
[2] J. H. Wu, R. S. Chang, and J. A. Jiang, *Sensors* **2007**, 7(12), 3366.
[3] K. Malinauskas, P. Palevicius, M. Ragulskis, V. Ostasevicius, and R. Dauksevicius, *Sensors* **2013**, 13(4), 5368.
[4] W. Zhou, B. Jing, D. Qu, G. Yuan, C. Wang, and H. Li, *Communication Systems and Information Technology*, Springer **2011**, 259.
[5] M. Golberg, J. Ruiz-Rivas, S. Polani, Y. Beiderman, and Z. Zalevsky, *Appl. Optics* **2018**, 57(7), B45 (2018).
[6] G. Joseph, A. Joseph, G. Titus, R. M. Thomas, and D. Jose, Proceedings of IEEE Conference on Emerging Research Areas: Magnetics, Machines and Drives, IEEE **2014**, 1.

[7] J. Liu, B. P. Y. Yan, W. X. Dai, X. R. Ding, Y. T. Zhang, N. Zhao, *Biomed. Opt. Express* **2016**, 7(10), 4313.
[8] D. Ruh, S. Subramanian, S. Sherman, J. Ruhhammer, M. Theodor, L. Dirk, K. Foerster, C. Heilmann, F. Beyersdorf, H. Zappe, A. Seifert, *Biomed. Opt. Express* **2016**, 7(9), 3230.
[9] C. Massaroni, C. Venanzi, A. P. Silvatti, D. L. Presti, P. Saccomandi, D. Formica, F. Giurazza, M. A. Caponero, E. Schena, *J. Biophotonics.* **2018**, 11(5), e201700263.
[10] T. Yang, X. Jiang, Y. Zhong, X. Zhao, S. Lin, J. Li, H. Zhu, *ACS sensors* **2017**, 2(7), 967.
[11] O. Vardoulis, T. S. Saponas, D. Morris, N. Villar, G. Smith, S. Patel, and D. Tan, *Med. Eng. Phys.* **2016**, 38(10), 1063.
[12] S. Hu, R. L. Bowlds, Y. Gu, and X. Yu, Proceedings of IEEE Conference on Engineering in Medicine and Biology Society, IEEE **2009**, 2312.
[13] H. Chang, and J. X. Chen, *Proceedings of Applied Informatics and Communication*, Springer **2011**, 541.
[14] C. Leitão, P. Antunes, J. Pinto, J. M. Bastos, and P. André, *Opt. Quant. Electron.* **2016**, 48(3), 218.
[15] M. Nishiyama, M. Sonobe, and K. Watanabe, *Biomed. Opt. Express* **2016**, 7(9), 3675.
[16] C. Leitão, P. F. da Costa Antunes, J. A. M. Bastos, J. de Lemos Pinto, and P. S. de Brito André, *IEEE Sens. J.* **2015**, 15(1), 14.
[17] Q. Sun, J. Wo, H. Wang, and D. Liu, Proc. SPIE **2014**, 9157, 91572K.
[18] J. Ma, H. Xuan, H. L. Ho, W. Jin, Y. Yang, and S. Fan, *IEEE Photon. Technol. Lett.* **2013**, 25(10), 932.
[19] H. Miyashita, *Curr. Hypertens. Rev.* **2012**, 8(2), 80.
[20] J. Wang, F. Ai, Q. Sun, T. Liu, H. Li, Z. Yan, D. Liu, *Opt. Express* **2018**, 26(19), 25293.
[21] L. Xu, M. Q. H. Meng, C. Shi, K. Wang, N. Li, *Acupunct. Med.* **2008**, 20(3), 175.
[22] R. Velik, *Eur. J. Integr. Med.* **2015**, 7(4), 321.
[23] L. Xu, M. Q. H. Meng, K. Wang, W. Lu, and N. Li, *Expert. Syst. Appl.* **2009**, 36(2), 3805.
[24] A. P. Avolio, M. Butlin, and A. Walsh, *Physiol. Meas.* **2009**, 31(1), R1.
[25] W. Wu, L. Yang, S. Zhang, D. Hao, Y. Yang, X. Li, and Z. Luo, *Comput. Aided. Surg.* **2016**, 21(sup1), 6.
[26] J. Song, S. Zhang, Y. Qiao, Z. Luo, J. Zhang, Y. Zeng, and L. Wang, *Eur. J. Obstet. Gynecol. Reprod. Biol.* **2004**, 117(2), 162.
[27] K. Meng, J. Chen, X. Li, Y. Wu, W. Fan, Z. Zhou, J. Yang, *Adv. Funct. Mater.* **2018**, 1806388.
[28] S. Mei, H. Gu, Q. Wang, S. Zhang, and Y. Zeng, J. *Obstet. Gynaecol. Re.* **2018**, 34(2), 179.
[29] H. Liu, D. Huang, S. Li, *J. Changchun Univ. Sci. Technol.* **2016**, 39(5), 139.
[30] F. Cai, C. Yi, S. Liu, Y. Wang, L. Liu, X. Liu, X. Xu, L Wang, L. *Biosens. Bioelectron.* **2016**, 77, 907.
[31] J. Blacher, S. Djane, R. Asmar, G. London, and M. Safar, *Am. J. Hypertens.* **1998**, 11(S4), 189A.